Journal of Alloys and Compounds 641 (2015) 155–161

Contents lists available at ScienceDirect

Journal of Alloys and Compounds

journal homepage: www.elsevier.com/locate/jalcom

Effects on the martensitic transformations and the microstructure of CuAlNi single crystals after ageing at 473 K

V.E.A. Araujo [a,*], R. Gastien [a], E. Zelaya [b,c], J.I. Beiroa [a], I. Corro [a], M. Sade [b,c,d], F.C. Lovey [b,d]

[a] Departamento de Investigaciones en Sólidos, CITEDEF, UNIDEF (MINDEF-CONICET), J.B. de La Salle 4397, (1603) Villa Martelli, Buenos Aires, Argentina
[b] División Física de Metales, Centro Atómico Bariloche–CNEA, S.C. Bariloche, Argentina
[c] Consejo Nacional de Investigaciones Científicas y Técnicas, Argentina
[d] Instituto Balseiro, Universidad Nacional de Cuyo, Argentina

ARTICLE INFO

Article history:
Received 19 January 2015
Received in revised form 7 April 2015
Accepted 9 April 2015
Available online 16 April 2015

Keywords:
Shape memory
Precipitation
Dislocations
Mechanical properties
Transmission electron microscopy, TEM

ABSTRACT

Isothermal treatments at 473 K were performed in CuAlNi single crystals to study their effects on the main properties of this shape memory material. Both the stress and thermally induced martensitic transformations were monitored after these ageing treatments. An increase of the critical transformation temperature was detected and the type of induced martensite changed from γ′ into β′ after a long enough ageing time. Pseudoelastic cycling was studied after thermal ageing; mechanical behaviour evolved on cycling and a repetitive behaviour was obtained after a small number of cycles. Changes in microstructure were analysed in the β phase by transmission electron microscopy which allowed observing the morphology and distribution of γ precipitates. The changes obtained in shape memory properties were discussed considering the atomic ordering evolution and characteristics of the precipitates.

1. Introduction

Shape memory alloys are useful materials in a large number of fields. Copper based alloys are particularly useful for actuator-based applications in cases where biocompatibility is not needed and low-cost devices can be designed for specific needs. Among copper based alloys, CuAlNi alloys are convenient when the actuator operates above room temperature.

Cu–14.3Al–4.1Ni (wt.%) alloys have a high temperature body centred cubic phase that after a quenching treatment can be obtained in a metastable state at room temperature [1]. During this quenching treatment, the bcc structure becomes an ordered structure type $L2_1$ named β in the following [2–4]. In some cases this order is not completed, and the ordering processes might continue if the material is thermally treated at temperatures high enough to allow diffusion. Depending on the ageing temperature, precipitation of γ phase could have an important role [5].

Martensitic transformations (MT) can be induced from this β phase. In fact, these phase transitions are responsible for the shape memory and pseudoelastic effects that characterise this type of materials. These transformations can be induced by cooling or by applying stress [1,6]. It is important to know if changes exist in these MT's after ageing the material at temperatures higher than room temperature. Many studies were carried out to analyse and control the shape memory response of Cu based alloys upon thermal treatments [7–9]. Previous work made by the present authors [10] shows that thermally and stress induced martensitic transformations are affected by isothermal treatments at 423 K. The effects obtained were most probably due to ordering processes than precipitation. Particularly, an increase in the critical transformation temperature was determined leading to an asymptotic behaviour after approx 100 h of thermal ageing at 423 K.

Other papers have focused their efforts on the evolution of Cu–Al–Ni after shorter thermal treatments [11,12] or studied by calorimetry [13,14]. The effects of submitting the material to long ageing treatments, as it would be if used as an actuator at these temperatures, have yet to be explored.

In the present manuscript, experimental results show the consequences of ageing treatments at 473 K. Three different aspects were analysed: the effect on the critical transformation temperatures and type of obtained martensite, the influence on the pseudoelastic effect and on pseudoelastic cycling, and the microstructural changes due to ageing which were determined mainly in the β phase by transmission electron microscopy.

2. Material and methods

Cu–14.3Al–4.1Ni (wt.%) alloys and single crystals were obtained as detailed in [8]. All single crystals were submitted to an initial heat treatment called Q which consisted in an annealing at 1203 K for 1 h and quenching in a mixture of water

* Corresponding author. Tel./fax: +54 11 4709 8228.
E-mail address: aaraujo@citedef.gob.ar (V.E.A. Araujo).

http://dx.doi.org/10.1016/j.jallcom.2015.04.065
0925-8388/

and ice to obtain β phase at room temperature. Samples subjected only to Q will be named "as quenched" in the following.

Ageing thermal treatments at 473 K during different time intervals were performed on samples (20 × 3 × 1) mm obtained from the single crystals and electrical resistance measurements were used to determine the characteristic temperatures M_s, M_f, A_s and A_f [2,8,15].

Round specimens for mechanical testing were prepared by mechanical and spark erosion (gage length 20 mm). These samples had a subsequent thermal treatment (Q type) to eliminate any possible effects caused by local heating of the sample during machining. After this heat treatment, their surfaces were mechanically and electrolytically polished. Tensile tests were carried out in an Instron 5567 machine with an Instron 3119-005 temperature chamber. Test details are described elsewhere [10].

The microstructure was observed by transmission electron microscopy (TEM) using a FEI CM200 operated at 200 kV. In order to determine the changes originated in the ageing treatments, the microstructure was analysed both in samples as quenched and samples after ageing treatments during several time periods at 473 K. To characterise the microstructure, TEM samples were prepared from the same single crystal used to prepare the tensile test specimens. Oval shaped slices of approximately (6 × 8 × 1) mm with surface normal close to the $[0\,0\,1]_\beta$ and $[1\,1\,0]_\beta$ direction were cut using a low speed diamond wheel saw. Determination of single crystal orientation was carried out with the Laue X-ray method. Once the ageing thermal treatment was performed, circular samples with 3 mm diameter were obtained by spark erosion and mechanically grinded to a thickness of 0.2 mm. Further thinning for TEM observation was performed by electropolishing using a TENUPOL double jet equipment. A 500 ml distilled water, 250 ml ethyl alcohol, 250 ml orthophosphoric acid, 50 ml propyl alcohol and 5 g urea solution was used as electrolyte at 12 V at 278 K.

3. Results and discussions

Results will be presented as follows. Firstly, an analysis of the changes in thermally and stress-induced martensitic transformations after thermal ageing treatments is presented. Secondly, the microstructure of the aged samples, analysed by TEM observations of the bulk, is compared with the obtained one in samples without ageing treatments. Finally, the characteristics of the microstructure are related to the behaviour of the thermally and stress induced martensitic transformations after ageing.

The effect of ageing treatments at 473 K on thermally induced martensitic (TIM) transformations was studied by measuring the electrical resistance of the samples and comparing the M_s temperature (martensite start temperature) before and after thermal treatments. Table 1 shows values of $\Delta M_s = M_s(t) - M_s(0)$ as a function of ageing time. $M_s(0)$ is the critical temperature M_s obtained for samples as quenched, and $M_s(t)$ are the values of M_s obtained after ageing each sample a time interval t at 473 K. Data obtained for three samples are shown in Fig. 1.

Table 1
Samples studied by electrical resistance measurements. ΔM_s represents the difference between the value of M_s for the sample as quenched and the value of M_s after some ageing time. Type of TIM indicates the type of temperature induced martensitic transformation obtained for the corresponding ageing time. The periods in column "ageing time" were selected to inform relevant changes observed.

Sample	Ageing time (h)	ΔM_s (K)	Type of TIM
R1	0	0	β ↔ γ′
	74	50	β ↔ β′
	194	57	β ↔ β′
R2	0	0	β ↔ γ′
	100	54	β ↔ β′
	190	52	β ↔ β′
R3	0	0	β ↔ γ′
	72	46	β ↔ β′
	213	57	β ↔ β′
R4	0	0	β ↔ γ′
	46	27	β ↔ γ′
	86	30	β ↔ β′ + γ′
	236	44	β ↔ β′
R5	0	0	β ↔ γ′
	41	23	β ↔ γ′
	101	34	β ↔ β′
	187	39	β ↔ β′

The thermally induced martensitic transformation is β ↔ γ′ in the as quenched state for this chemical composition, which was confirmed in every analysed sample. Two different aspects should be mentioned here. On one hand, the critical transformation temperature does change after ageing treatment. On the other hand, the type of induced martensite changes after a period of ageing time. Considering the first point, after ageing treatments the behaviour of the TIM transformations might be considered as formed by two stages. In the first one, ΔM_s increases an amount between 30 K and 50 K while in the second stage an asymptotic behaviour is observed. The asymptotic behaviour starts after approximately 60 h and the longest analysed time interval was 200 h. Moreover, the martensitic transformation changes from β ↔ γ′ to β ↔ β′ after ageing intervals longer than 60 h. After this change of type of martensitic transformation, nearly no variation of M_s is detected. An example of this behaviour, observed in each sample, is shown in Fig. 2 for sample R1. In some cases, a mixed type transformation β ↔ γ′ + β′ has been also obtained.

It is interesting to notice that the value of M_s can be modified by ageing treatments without losing the main characteristics of the thermally induced martensitic transformation. This would allow the selection of different thermal treatments, using the same chemical composition, to approach the design characteristics required for actuators. Additionally, the decrease in the hysteresis width due to the change of martensite might be an advantage for actuator-based devices.

Regarding the stress induced martensitic transformations (SIM transformations), only the β ↔ β′ martensitic transition was analysed. As it was reported, critical stresses to induce the β ↔ β′ pseudoelastic cycles are more repetitive in comparison with required stresses to induce the β ↔ γ′ transformation [16]. This MT also has a small hysteresis width which is an asset when designing actuators if compared with the β ↔ γ′ transition. After ageing treatments which do not alter the type of thermally induced martensite, test temperature must be at least 30 K higher than the M_s temperature in order to obtain stress induced β′ martensite. Keeping this fact in mind, critical stresses to induce the β′ martensite were measured and in all cases a decrease was obtained if compared with those samples as quenched. Fig. 3(a) shows a plot of transformation and retransformation stresses as a function of ageing time. These stresses were taken from pseudoelastic cycles performed at 323 K after different ageing time intervals as the ones

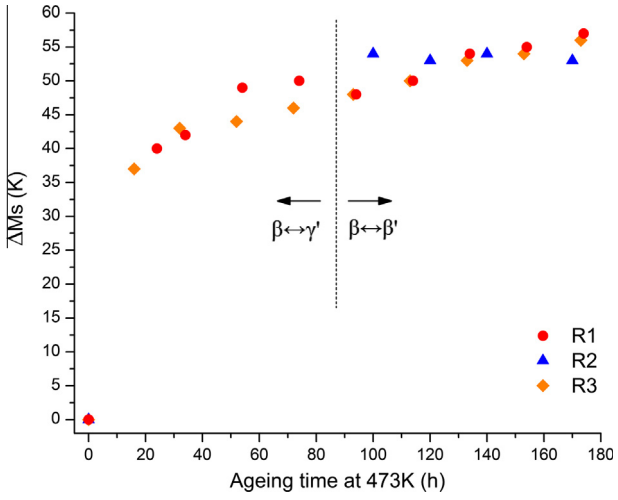

Fig. 1. ΔM_s vs. ageing time at 473 K for samples R1, R2 and R3. The dashed line indicates the change in martensitic transformation for samples R1 and R2.

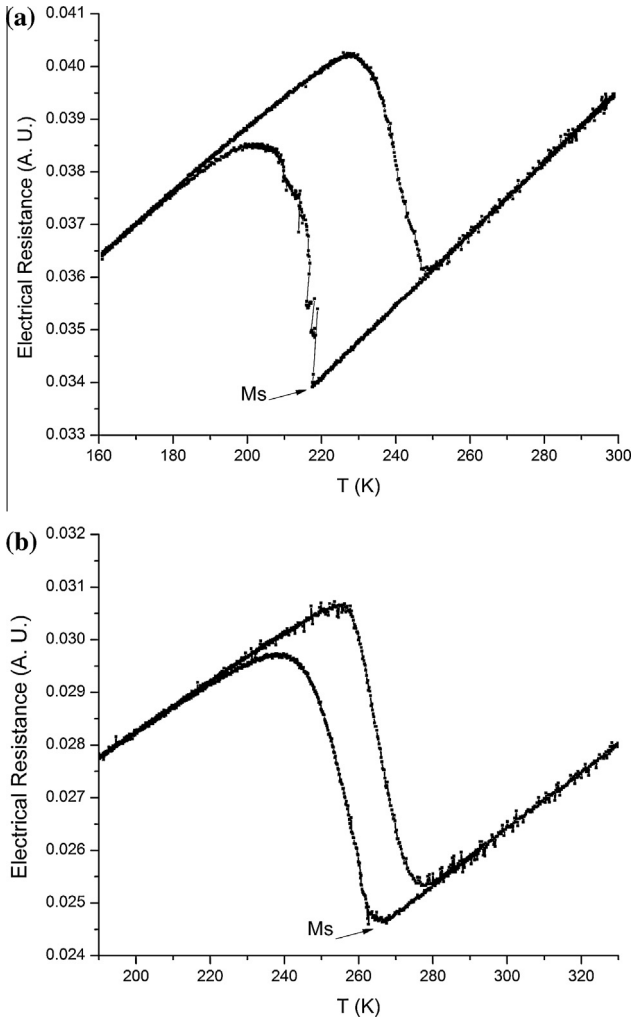

Fig. 2. (a) Electrical resistance vs. temperature cycle made on sample R1 as quenched showing a $\beta \leftrightarrow \gamma'$ type transformation. (b) Electrical resistance vs. temperature cycle made on R1 after 74 h at 473 K.

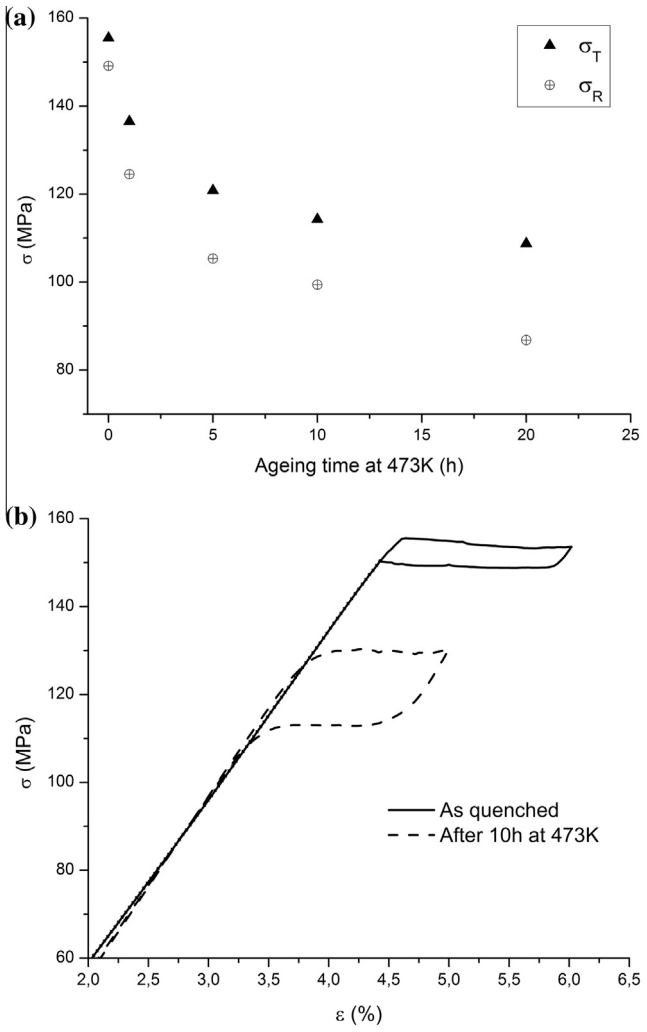

Fig. 3. (a) Transformation stresses (σ_T) and retransformations stresses (σ_R) vs. ageing time at 473 K. All pseudoelastic cycles are $\beta \leftrightarrow \beta'$ transitions performed at 323 K. Load axis orientation: [5 1 16]. (b) Pseudoelastic $\beta \leftrightarrow \beta'$ cycle for sample as quenched and pseudoelastic $\beta \leftrightarrow \beta'$ cycle with larger hysteresis width after 10 h of ageing time at 473 K. Both cycles were performed at 323 K.

shown in Fig. 3(b). There is a decrease in critical stresses that does not occur equivalently for transformation and retransformation. Thus, an increase in hysteresis width is present with ageing time. The hysteresis width for the cycles performed at the same temperature is three times larger after 5 h at 473 K than the one observed for the cycle without ageing.

Pseudoelastic $\beta \leftrightarrow \beta'$ cycling was performed in samples detailed in Table 2. Ageing time on these samples was short enough that the TIM remained $\beta \leftrightarrow \gamma'$ and testing temperatures were selected to obtain $\beta \leftrightarrow \beta'$ as a SIM transformation.

Fig. 4 shows stress–strain curves of selected cycles obtained for sample C1. On one hand, it can be noted that the critical stress decreases in the first cycles but after these first cycles (approx. 100 cycles) it maintains nearly constant. On the other hand, the critical stress for retransformation is nearly constant during all cycling. Consequently, the hysteresis width decreases in these first cycles. In order to better illustrate this behaviour, the graph in Fig. 5 shows critical stresses for transformation and retransformation for the same sample as a function of the number of cycles N. The difference between the critical stress for cycles $N = 100$ and $N = 500$ is near 0.7%. This value can be considered negligible.

In order to understand the origin of this behaviour, the microstructure of samples listed in Table 3 was analysed. As a first point the microstructure of samples as quenched is analysed.

Table 2
Samples subjected to pseudoelastic cycling. The number next to the C indicates the different single crystals used.

Sample	Ageing time at 473 K (h)	Number of pseudoelastic cycles (N)	Axis orientation	Test temperature (K)
C1	25	1000	[100]	325
C2	25	1000	[732]	263
C3	42	1000	[504]	323

Fig. 6(a) shows a low magnification bright field image in $[0\,0\,1]_\beta$ zone axis of M1 (as quenched). The micrograph was taken in two beam condition using (2 2 0) spot. As observed, around 50% of the dislocations have the lines parallel to $[1\,0\,0]_\beta$ or $[0\,1\,0]_\beta$ directions. Moreover, the bright field of the same area in two beam condition using (4 0 0) spot shows the extinction of dislocations with the line parallel to $[0\,1\,0]_\beta$ direction. These dislocations are pointed out with dashed line arrows in Fig. 6(a) and (b). On the other hand using the (0 4 0) spot for two beam condition, the dislocations with the lines parallel to $[1\,0\,0]_\beta$ extinguished (Fig. 6(c)). However, the

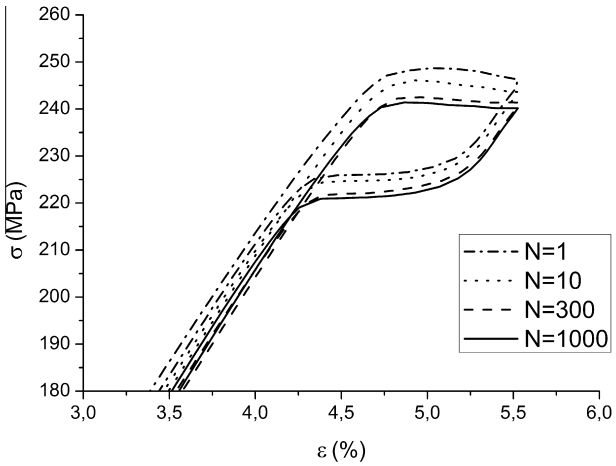

Fig. 4. (a) Pseudoelastic β ↔ β′ cycles for N = 1, 10, 300 and 1000 of sample C1 aged 25 h at 473 K.

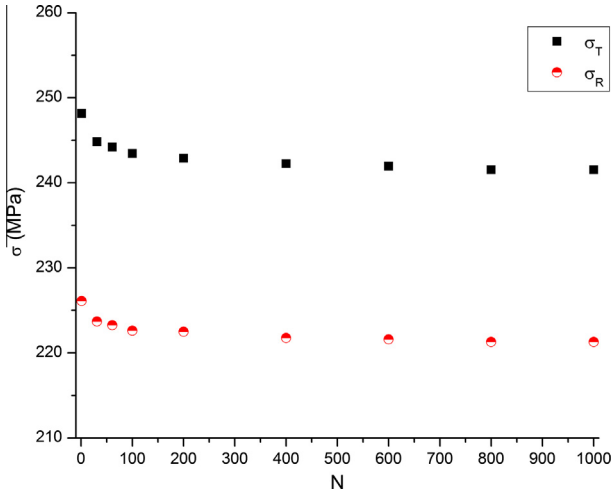

Fig. 5. Transformation and retransformation critical stresses vs. N (number of cycle) for β ↔ β′ cycling of sample C1 after 25 h at 473 K.

Table 3
Samples observed by transmission electron microscopy. The number next to M indicates the different samples used. S is the standard deviation for the diameter of γ precipitates.

Sample	Ageing time at 473 K (h)	Average diameter of γ precipitates (nm)	S (nm)
M1	0	–	
M2	26	42.2	11.2
M3	25	47.1	10.8
M4	42	61.5	15.5
M5	50	29.9	7.8
M6	50	83.6	12.0
M7	100	97.1	28.4
M8	150	72.9	16.8

dislocations having the lines directions inclined with respect to both the [1 0 0] and the [0 1 0] directions do not extinguish. Since the β phase in Cu based alloys is rather elastically anisotropic, these extinctions criteria only occur for particular cases: when the line direction is perpendicular to a symmetry plane of the structure and the direction vector of the diffracting vector is perpendicular to both the line direction and the Burgers vector. Hence, we can ensure that the dislocations extinguished in Fig. 6(b) and (c) are edge dislocations with Burgers vectors parallel to the [1 0 0] and the [0 1 0] directions respectively. The same behaviour was observed in Cu–Zn–Al–Ni alloys quenched with a similar heat treatment to Q [17,18]. The invisibility criterion $\bar{g} \cdot \bar{b} = 0$ and $\bar{g} \cdot (\bar{b} \times \bar{u}) = 0$ was used to obtain the direction of the burgers vector $\bar{b}$, with $\bar{g}$ being the reflecting vector and $\bar{u}$ the dislocation line. This kind of contrast is consistent with one dislocation $\bar{b} = a/2[0\,0\,1]$, where a is the lattice parameter of the $L2_1$ structure. It could also be appreciated in this case and in the cited work [17,18] that most of the of the dislocations pointed with arrows have a double line.

After analysing the material in the as quenched state, the microstructure of the aged samples was studied. Fig. 7(a) shows a typical bright field image of sample M7 along [1 1 0] zone axis. Here, four precipitates with darker contrast than the β matrix can be appreciated. An EDS measurement performed over the precipitate, indicated with a grey dashed line arrow, shows ∼5%at Al more than the matrix next to it, pointed with a black full line arrow. The same amount of Al increment was observed in the precipitates respect to the matrix in 20 different precipitates. The increment of Al content in the precipitates agrees with the presence of γ phase. Moreover, the SAD taken over an area with precipitates could be indexed according β and γ phase in [1 1 0] direction.

In Fig. 8(a) and (b), bright field images can be observed on sample M4 with different magnifications. The low magnification micrograph shows the tendency of the precipitates to accommodate along defined lines (Fig. 8(a)). By tilting the sample, it was always distinguished the presence of dislocations under the precipitates lines. However, there are still some dislocations without any precipitates nearby (Fig. 8(b)). Precipitates seem to prefer growing along dislocations in [1 0 0] directions. Fig. 8(c) and (d) show bright field images of sample M7. The low magnification micrograph of this sample shows the same tendency of the precipitates to group over dislocations lines. When comparing this sample with sample M4, an increment of the number of precipitates could be detected (Fig. 8(a) and (c)). Fig. 8(d) shows magnified area of M7. As it could be observed in this micrograph, the number of precipitates per area and the size of them seem to increase in comparison to Fig. 8(b). It is also observed in Fig. 8(d) that most of the precipitates accommodated with the sharp borders parallel to each other. It should also be pointed out that no dislocations were found free of precipitates in this sample.

The nucleation near dislocations could be explained taking into account the main differences between both involved phases (β and the precipitates). The γ phase possesses two vacancies in the unit cell. In Ref. [12], it is suggested that dislocations could be a better source for vacancies needed to nucleate the γ phase in the β matrix. However, Zárubová et al. [12] did not analyse the size evolution of precipitates or TIM transitions since they only study the changes after 30 min at 473 K. In this work, we found that the average diameter of precipitates does not change significantly with increasing ageing time (Table 3) and the saturation of dislocations with precipitates after 60 h of ageing (Fig. 8) could be related to the two stages of the TIM transformations described in Fig. 1.

The accommodation with the sharp borders parallel to each other sharing $\{1\,0\,0\}_\beta$ type planes could be explained due to a minimization of elastic interaction energy of precipitates with this configuration [19]. Furthermore, in the first stage precipitates seem to accommodate near border dislocations lying in [1 0 0] in order to decrease stresses created in the edge of those dislocations. This is possible due to the fact that precipitates have a smaller cell volume than the β phase.

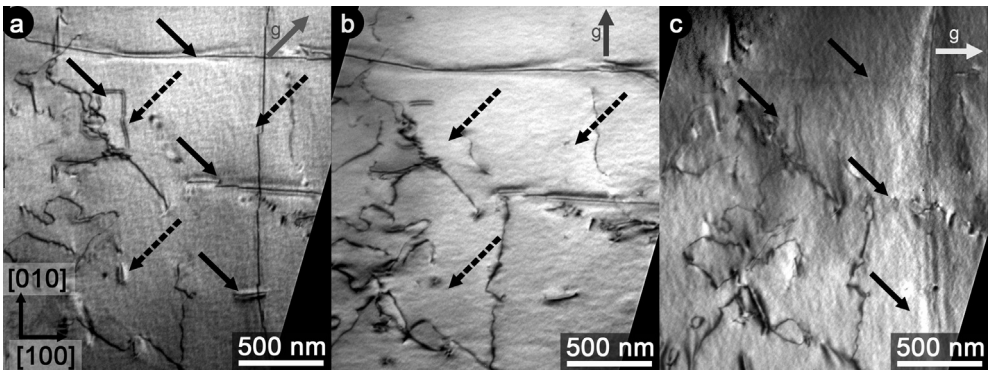

Fig. 6. Bright field images of sample as quenched in $[0\,0\,1]_{\beta}$ zone axis. (a) Micrograph in two beam condition using (2 2 0) spot. (b) Micrograph in two beam condition using (0 4 0) spot. (c) Micrograph in two beam condition using (4 0 0) spot.

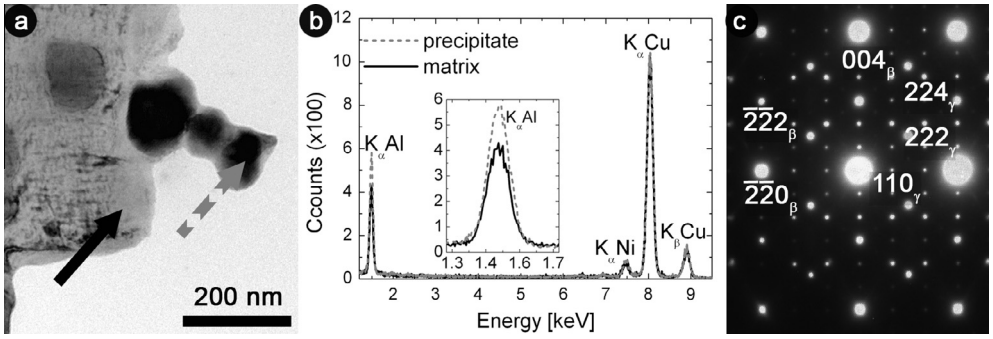

Fig. 7. (a) Bright field image of sample aged 100 h at 473 K in $[1\,1\,0]_{\beta}$ zone axis. (b) EDS of the precipitate pointed with the grey dashed line arrow in (a) and the matrix next to it pointed with the full line black arrow. The inset shows the increment of Al in the γ phase precipitate. (c) SAD pattern of the same sample in $[1\,1\,0]_{\beta}$.

It is clear after revising the microstructural evidence that γ precipitates should have a more important role in affecting the TMs for this kind of longer ageing treatments at 473 K. The precipitation of γ phase can change the martensite induced and increase transformation temperatures by producing regions of lower aluminium content in the β matrix [20] which correlates well with the results presented. However, ordering processes can also cause the M_s to increase at least for ageing treatments of less than 40 h [11,14].

Volume density of precipitates was calculated assuming that the sample had constant thickness (approx. 120 nm) and that dislocations had all the lines covered with precipitates. Results revealed that the volume fraction of the γ phase would be always lower than 0.7%. This assessment was made by considering that no significant size evolution of the precipitates is observed as ageing time grows, as shown in Table 3. Thus, the average diameter of γ precipitates was calculated as the mean value of all the samples showed in Table 3. In consequence, the aluminium content that the precipitates took from the β matrix could not justify an M_s shift as large as the one calculated from electrical resistance measurements [20]. This would indicate that the driving force behind the changes in transformation temperatures is an increase in the degree of order in the matrix.

The reason that the transformation changes from $\beta \leftrightarrow \gamma'$ to $\beta \leftrightarrow \beta'$ could be that the precipitates generate a barrier for the γ' nucleation, in the same way as the presence of dislocations finally caused the γ' inhibition in $\beta \leftrightarrow \beta' + \gamma'$ cycling [21]. This effect basically occurs because of the twin related nature of γ' martensite. In this case, the precipitates would interact differently with each twinned γ' variant, generating an energetic unbalance that makes the creation of an undistorted habit plane difficult, finally causing an inhibition of this martensitic structure. This is not the case of β' martensite which has non twinned related variants and could be nucleated instead of γ' martensite.

In reference to the SIM transformations, an increase in the degree of order in the matrix can be responsible for the decrease in critical stresses. However, the growth of hysteresis width is usually associated with the presence of precipitates in the matrix [22,23]. Both consequences have been observed for the same alloy subjected to longer ageing treatments at 423 K [10].

Aged samples were studied by TEM after being subjected to pseudoelastic cycling. In Fig. 9, it can be observed that dislocations are located around the γ precipitates generated during ageing. The mechanism by which accumulation of dislocations after cycling occurs in zones free of precipitates [21] is not present here. Instead, the great amount of dislocations blurs the edge of the precipitates (Fig. 9(b)). On the contrary, this kind of defects around γ precipitates are not observed in the aged sample that was not cycled (Fig. 9(a)). This fact would indicate that the dislocations were created during cycling and their location can help to explain the effect illustrated in Fig. 5. During the first cycles, more energy is needed to accommodate dislocations around the γ precipitates. Furthermore, these dislocations seem to collaborate with the deformation caused by the martensite around the precipitates. After a sufficient amount of defects is created, the deformation of the material requires less energy. In consequence, the transformation stress and the hysteresis width become constant at lower values. This effect was also observed in other Cu-based shape memory alloys [23,24].

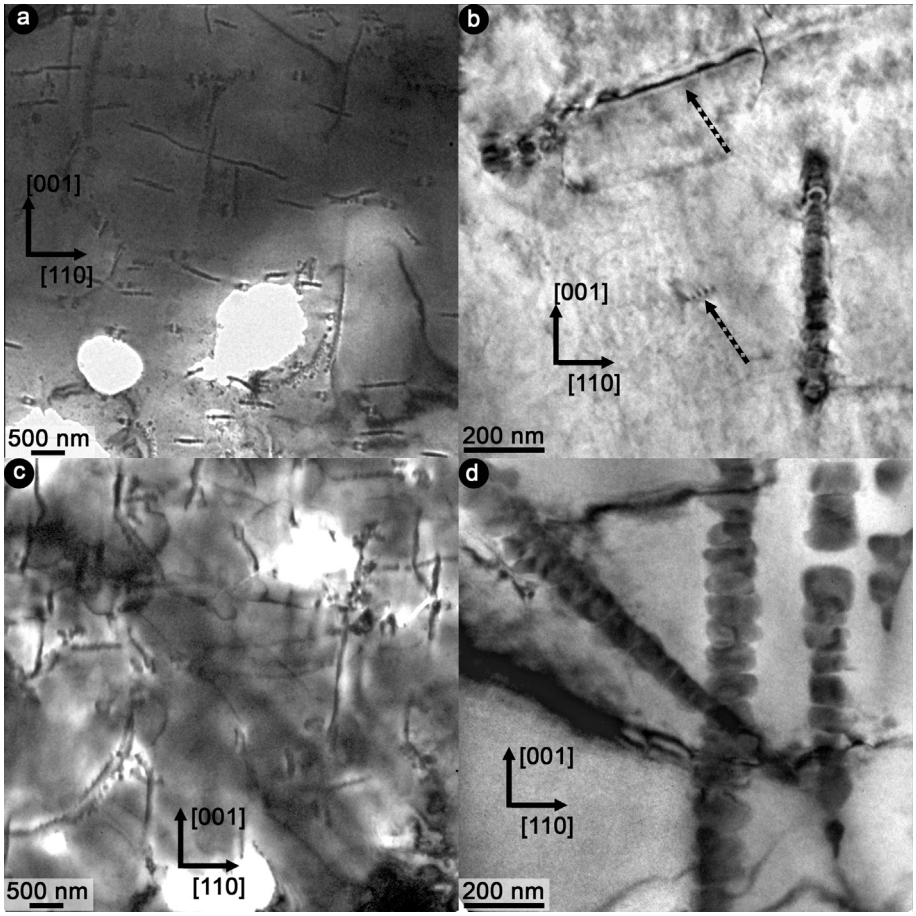

Fig. 8. Bright field images of samples aged 42 h at 473 K (a and b) and 100 h at 473 K (c and d) with low and high magnification in $[1\ 1\ 0]_{\beta}$ zone axis. Dislocations without precipitates are pointed with dashed line arrows in (b).

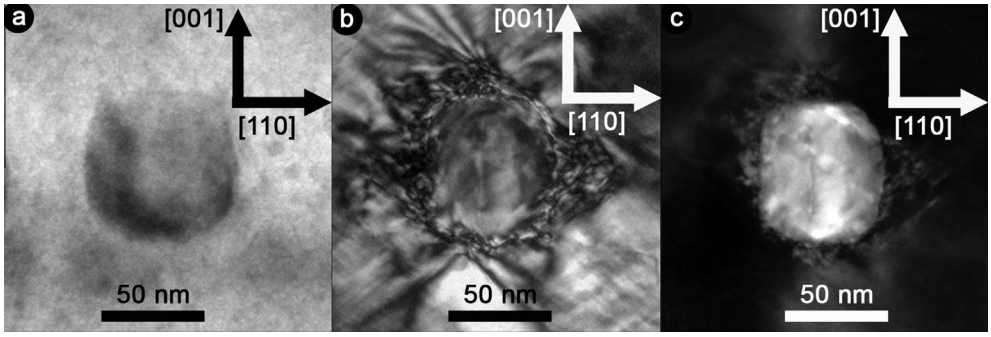

Fig. 9. (a) Bright field image of a γ precipitate in sample aged 42 h at 473 K. (b) Bright field image of a γ precipitate in sample aged 42 h at 473 K and cycled 1000 times surrounded by dislocations generated during pseudoelastic cycling. (c) Dark field image of a γ precipitate in the same sample as (b).

4. Conclusions

The effects after thermal ageing at 473 K on the martensitic transformations in CuAlNi single crystals were analysed.

TIM transformations revealed changes upon ageing that can be divided in two stages as ageing time increases: a first rise in critical temperatures and a subsequent asymptotic behaviour with a change of the type of martensite induced. Longer ageing treatments allow, for this chemical composition, selecting the M_s temperature and the type of transformation needed for an application.

The SIM transformations behaviour after ageing was analysed for the $\beta \leftrightarrow \beta'$ transformation where a decrease in critical stresses and an increase in hysteresis width were observed. Pseudoelastic $\beta \leftrightarrow \beta'$ cycling was performed after thermal ageing. An evolution took place in the first cycles and then a repetitive behaviour was obtained which can be very useful in the design of actuators.

As concerns the microstructure, ageing generates an inhomogeneous distribution of γ precipitates nucleated at dislocations and an increase in the degree of order in the β matrix. The precipitates have visible effects like an increase in hysteresis width in pseudoelastic cycles. The small volume fraction of γ phase indicated that the modification of the degree of order also could play an important role in changing parameters of martensitic transformations for ageing at 473 K. A decrease in critical stresses and the growth of the M_s value were related to this modification.

Acknowledgements

The authors thank C. Gómez Bastidas for his help in single crystal growth, P. Riquelme for his technical support in mechanical tests, C.E. Corbellani for her help in sample preparation and crystal orientation determinations and M.R. Esquivel for revising the manuscript. The financial support from ANPCyT (PICT 2012-0884), Universidad Nacional de Cuyo (06/C452.), CONICET (PIP 112 2011 0100 513) and SCTP-Ministerio de Defensa (PIDDEF 015/11) are gratefully acknowledged.

References

[1] K. Otsuka, H. Sakamoto, K. Shimizu, Successive stress-induced martensitic transformations and associated transformation pseudoelasticity in Cu–Al–Ni alloys, Acta Metall. 27 (1979) 585–601.
[2] V. Recarte, O.A. Lambri, R.B. Pérez-Sáez, M.L. Nó, J. San Juan, Ordering temperatures in Cu–Al–Ni shape memory alloys, Appl. Phys. Lett. 70 (1997).
[3] J.I. Pérez-Landazábal, V. Recarte, R.B. Pérez-Sáez, M.L. Nó, J. Campo, J. San Juan, Determination of the next-nearest neighbor order in β phase in Cu–Al–Ni shape memory alloys, Appl. Phys. Lett. 81 (2002).
[4] Y. Nakata, T. Tadaki, K. Shimizu, Site determination of Ni atoms in Cu–Al–Ni shape memory alloys by electron channelling enhanced microanalysis, Mater. Trans. JIM 31 (1990) 652–658.
[5] D.P. Dunne, N.F. Kennon, Ageing of copper-based shape memory alloys, Met. Forum 4 (1981) 176–183.
[6] R. Gastien, C.E. Corbellani, H.N. ÁlvarezVillar, M. Sade, F.C. Lovey, Pseudoelastic cycling in Cu–14.3Al–4.1Ni (wt.%) single crystals, Mater. Sci. Eng. A 349 (2003) 191–196.
[7] N.F. Kennon, D.P. Dunne, L. Middleton, Aging effects in copper-based shape memory alloys, Metall. Trans. A 13 (1982) 551–555.
[8] R. Gastien, C.E. Corbellani, P.B. Bozzano, M.L. Sade, F.C. Lovey, Low temperature isothermal ageing in shape memory CuAlNi single crystals, J. Alloys Comp. 495 (2010) 428–431.
[9] D.O. Roqueta, F.C. Lovey, M. Sade, Hysteresis evolution in the martensitic transformation cycling in β-Cu–Zn–Al samples with γ-phase precipitates, Scr. Mater. 36 (1997) 385–391.
[10] R. Gastien, C.E. Corbellani, V.E.A. Araujo, E. Zelaya, J.I. Beiroa, M. Sade, F.C. Lovey, Changes of shape memory properties in CuAlNi single crystals subjected to isothermal treatments, Mater. Charact. 84 (2013) 240–246.
[11] V. Recarte, R.B. Pérez-Sáez, M.L. Nó, J. San Juan, Evolution of martensitic transformation in Cu–Al–Ni shape memory alloys during low-temperature aging, J. Mater. Res. 14 (1999) 2806–2813.
[12] N. Zárubová, A. Gemperle, V. Novak, Initial stages of y2 precipitation in an aged Cu–Al–Ni shape memory alloy, Mater. Sci. Eng. A 222 (1997) 166–174.
[13] J.I. Pérez-Landazábal, V. Recarte, V. Sánchez-Alarcos, Influence on the martensitic transformation of the β phase decomposition process in a Cu–Al–Ni shape memory alloy, J. Phys. Condens. Matter 17 (2005) 4223–4236.
[14] J. Van Humbeeck, D. Van Hulle, L. Delaey, J. Ortín, C. Seguí, V. Torra, A two-stage martensite transformation in a Cu–13.99 mass% Al–3.5 mass% Ni alloy, Trans. Jpn. Inst. Met. 28 (1987) 383–391.
[15] M. Sade, J.L. Pelegrina, A. Yawny, F.C. Lovey, Diffusive phenomena and pseudoelasticity in Cu – Al – Be single crystals, J. Alloys Comp. 622 (2015) 309–317.
[16] R. Gastien, C.E. Corbellani, M. Sade, F.C. Lovey, Thermal and pseudoelastic cycling in Cu–14.1–Al–4.2Ni (wt%) single crystals, Acta Mater. 53 (2005) 1685–1691.
[17] E. Zelaya, J.L. Pelegrina, M. Ahlers, Quenching and ageing behaviour of quaternary Cu–Zn–Al–Ni single crystals, J. Phys. IV 11 (2001) 147–152.
[18] G.D. Serrano, J.L. Pelegrina, a.M. Condó, M. Ahlers, Helical dislocations as vacancy sinks in β phase Cu–Zn–Al–Ni alloys, Mater. Sci. Eng. A 433 (2006) 149–154.
[19] T. Miyazaki, H. Imamura, H. Mori, T. Kozakal, Theoretical and experimental investigations on elastic interactions between γ′-precipitates in a Ni–Al alloy, J. Mater. Sci. 16 (1981) 1197–1203.
[20] V. Recarte, R.B. Pérez-Sáez, E.H. Bocanegra, M.L. Nó, J. San Juan, Dependence of the martensitic transformation characteristics on concentration in Cu – Al – Ni shape memory alloys, Mater. Sci. Eng. A 273–275 (1999) 380–384.
[21] R. Gastien, M. Sade, F.C. Lovey, Interaction between martensitic structure and defects in β↔β'+γ' cycling in CuAlNi single crystals. Model for the inhibition of γ′ martensite, Acta Mater. 56 (2008) 1570–1576.
[22] D.O. Roqueta, F.C. Lovey, M. Sade, Martensite-austenite stability shifts due to the presence of γ-phase precipitates in Cu–Zn–Al alloys, Scr. Mater. 40 (1999) 1359–1365.
[23] F.C. Lovey, V. Torra, A. Isalgué, D. Roqueta, M. Sade, Interaction of single variant martensitic transformation with small γ type precipitates in Cu–Zn–Al, Acta Metall. Mater. 42 (1994) 453–460.
[24] D. Roqueta, F.C. Lovey, M. Sade, The hysteresis in the martensitic transformations due to the interaction with precipitates in Cu–Zn–Al alloys, Scr. Mater. 34 (1996) 1747–1752.